

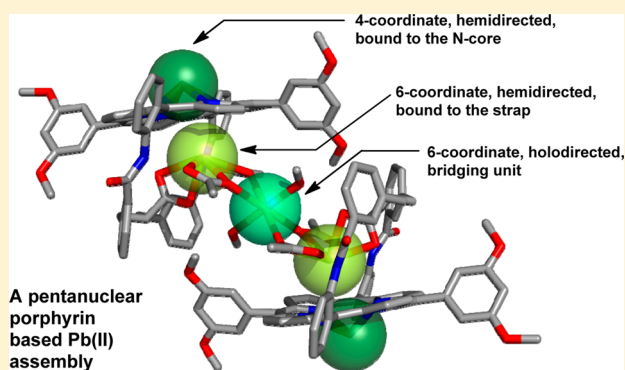
A Pentanuclear Lead(II) Complex Based on a Strapped Porphyrin with Three Different Coordination Modes

Stéphane Le Gac,* Eric Furet, Thierry Roisnel, Ismail Hijazi, Jean-François Halet,* and Bernard Boitrel*

Institut des Sciences Chimiques de Rennes, UMR 6226, CNRS - Ecole Nationale Supérieure de Chimie de Rennes—Université de Rennes 1, F-35042 Rennes Cedex, France

Supporting Information

ABSTRACT: We have previously described Pb(II) and Bi(III) bimetallic complexes with overhanging carboxylic acid strapped porphyrins in which one metal ion is bound to the N-core (“out-of-plane”, OOP), whereas the second one is bound to the strap (“hanging-atop”, HAT). In such complexes, the hemidirected coordination sphere of a HAT Pb(II) cation provides sufficient space for an additional binding of a neutral ligand (e.g., DMSO). Interestingly, investigations of the HAT metal coordination mode in a single strap porphyrin show that a HAT Pb(II) can also interact via intermolecular coordination bonds, allowing the self-assembly of two bimetallic complexes. In the pentanuclear Pb(II) complex we are describing in this Article, three different coordination modes were found. The OOP Pb(II) remains inert toward the supramolecular assembling process, whereas the HAT Pb(II) cation, in addition to its intramolecular carboxylate and regular exogenous acetate groups, coordinates an additional exogenous acetate. These two acetates are shared with a third lead(II) cation featuring a holo-directed coordination sphere, from which a centro-symmetric complex is assembled. Density functional theory calculations show some electron-density pockets in the vicinity of the hemidirected HAT Pb(II) atoms, which are associated with the presence of a stereochemically active lone pair of electrons. On the basis of the comparison with other HAT Pb(II) and Bi(III) systems, the “volume” of this lone pair correlates well with the bond distance distributions and the number of the proximal oxygen atoms tethered to the post-transition metal cation. It thus follows the order 6-coordinate Bi(III) > 6-coordinate Pb(II) > 5-coordinate Pb(II).



INTRODUCTION

Coordination chemistry of either bismuth(III) or lead(II) cations remains largely unexplored in porphyrin platform-based ligands.^{1,2} As a result, structural data available are limited to a few examples.³ However, because they possess a stereochemically active $6s^2$ lone pair, both of these elements are expected to exhibit some similarities in their coordination properties.^{4,5} For a decade now, our group has been investigating the influence of various types of functionalities such as pendant pickets or crown-ethers around the coordination site of the macrocycle on its coordination properties.⁶ Among them, the so-called overhanging carboxylic acid porphyrins possess a very peculiar behavior, with a possible control of both the kinetics of metal insertion and the nuclearity of the resulting complex.⁷ In contrast with the previous chelators,⁸ this series of ligands consists of single or bis-strapped porphyrins in which a carboxylic acid group is hanging from a true apical position over the coordination site.⁹ This type of geometry is quite different from other porphyrin platforms previously reported by Chang et al.¹⁰ or later by Nocera et al.¹¹ in which the carboxylic acid is located at a more lateral position. In the case of one porphyrin of this series (**2**), both X-ray structures of a mononuclear bismuth complex **2_{Bi}**¹² and an unprecedented C_2 -symmetrical

dinuclear lead complex **2Pb₂** (see Figure 1, top) were initially resolved.¹³ A typical characteristic of this type of ligands is the propensity to incorporate a metal ion almost instantaneously at room temperature under mild conditions by means of a deconvolution process of the metal salt to which the overhanging carboxylic acid participates. Furthermore, we have shown that this deconvolution step led, in the presence of a metal bound out-of-plane (OOP), to the macrocycle and, under specific and controlled conditions, to new dinuclear complexes in which the two metals can undergo a degenerate exchange reaction (double translocation process).^{14,15} Among various bimetallic complexes¹⁶ were obtained for instance the dinuclear lead(II) complex **1_{Pb}·PbOAc** from a single strapped porphyrin,¹⁷ the heterobimetallic complex **2_{Bi}·PbOAc** from the bis-strapped analogous compound, as well as the dinuclear bismuth(III) complex **2_{Bi}·Bi(OAc)₂** (see Figure 1, bottom).¹⁴

In these three complexes, two different coordination modes coexist: the regular out-of-plane (OOP) coordination mode and the so-called hanging-atop one (HAT) that reflects the fact that the metal is hanging from the intramolecular carboxylate

Received: July 25, 2014

Published: September 11, 2014

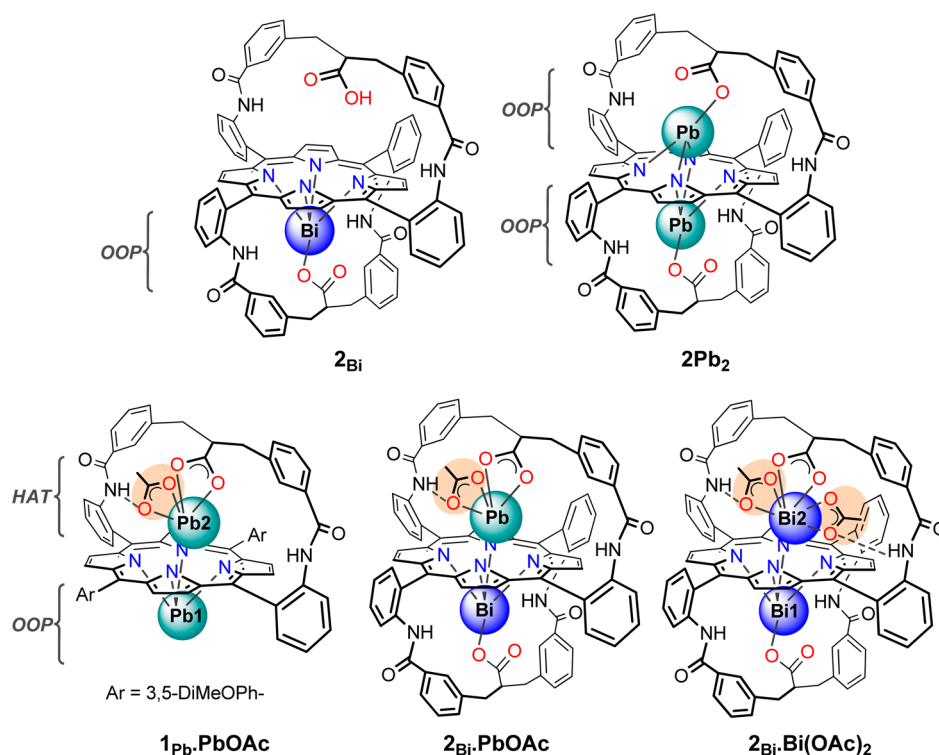


Figure 1. Background of known lead and bismuth complexes from overhanging carboxylic acid porphyrins. Top: 2_{Bi} (left) and 2_{Pb_2} (right) exhibiting only OOP (out-of-plane) coordination of the cations. Bottom: $1_{\text{Pb}} \cdot \text{PbOAc}$, $2_{\text{Bi}} \cdot \text{PbOAc}$, and $2_{\text{Bi}} \cdot \text{Bi}(\text{OAc})_2$ incorporating both OOP and a HAT (hanging-atop) cations.

group without any bonding to the N-core of the macrocycle. In the HAT coordination, the presence of either one or two H-bonds between the exogenous acetate group(s) bound to the metal and the amide group(s) from the strap is essential (dashed lines in Figure 1). Additionally, upon complexation of a HAT metal ion, it appears that the strap is significantly shifted from the apical position, leading to an open space for potential additional interactions with the metal. Contrary to bismuth(III), which is surrounded by three counterions, the intramolecular carboxylate and two exogenous acetate moieties, lead(II) is surrounded by two counterions, and a weakly bound solvent molecule (DMSO is commonly observed in the solid state). On the basis of the exchange of this last coordination, new types of supramolecular edifices could be obtained through interaction with bridging ligands. As such, we describe here the solid-state structure of an unprecedented supramolecular assembly of two dinuclear lead porphyrin complexes derived from $1_{\text{Pb}} \cdot \text{PbOAc}$, via a fifth lead cation bridging two HAT Pb(II). Remarkably, three different coordination modes are present in this supramolecular edifice. Moreover, the HAT Pb(II) cations have coordination spheres very similar to that of the HAT Bi(III) cation in complex $2_{\text{Bi}} \cdot \text{Bi}(\text{OAc})_2$ depicted in Figure 1 (i.e., 6-coordinate with three COO^- ligands). Thus, DFT calculations have been performed to evaluate and compare the $6s^2$ lone pair of electrons on this type of structure.

EXPERIMENTAL SECTION

Preparation of Single Crystals of $[1_{\text{Pb}} \cdot \text{Pb}(\text{OAc})_2]_2 \text{Pb}(\text{MeOH})_2$ for X-ray Crystallography Study. Ligand **1** (20 mg) was dissolved in pyridine, 5 equiv of lead acetate was added, and the mixture was stirred for 3 h at room temperature. The metalation reaction was monitored by UV–vis spectroscopy. After the completion of the reaction, pentane was added until precipitation of a greenish solid. The residue was redissolved in chloroform, and methanol was added in a

sealed tube to allow slow diffusion in the chloroform solution, which led to single crystals suitable for X-ray diffraction study. $\text{C}_{142}\text{H}_{112}\text{N}_{12}\text{O}_{26}\text{Pb}_5$, $4(\text{CHCl}_3)$; $M_w = 3915.86$. APEXII, Bruker-AXS diffractometer, Mo K_α radiation ($\lambda = 0.71073 \text{ \AA}$), $T = 150(2) \text{ K}$; triclinic $\overline{P}1$ (I.T. #2), $\beta = 2990(10)$, $a = 13.9076(3)$, $b = 15.3898(3)$, $c = 18.0075(4) \text{ \AA}$, $\alpha = 68.6250(10)^\circ$, $\gamma = 84.6290(10)^\circ$, $V = 3573.02(13) \text{ \AA}^3$, $Z = 1$, $d = 1.82 \text{ g cm}^{-3}$, $\mu = 6.170 \text{ mm}^{-1}$. The structure was solved by direct methods using the SIR97 program,¹⁸ and then refined with full-matrix least-squares methods based on F^2 (SHELXL-97)¹⁹ with the aid of the WINGX program.²⁰ All non-hydrogen atoms were refined with anisotropic atomic displacement parameters. H atoms were finally included in their calculated positions. A final refinement on F^2 with 16 283 unique intensities and 907 parameters converged at $\omega R(F^2) = 0.1218$ ($R(F) = 0.0527$) for 12 169 observed reflections with $I > 2\sigma(I)$. CCDC-923915 contains the supplementary crystallographic data for this structure. These data can be obtained free of charge at www.ccdc.cam.ac.uk/conts/retrieving.html [or from the Cambridge Crystallographic Data Centre, 12, Union Road, Cambridge CB2 1EZ, UK; fax, +44-1223-336-033; e-mail, deposit@ccdc.cam.ac.uk].

Theoretical Calculations. Density functional theory (DFT) calculations were performed using the ADF2012.01 (Amsterdam Density Functional) package.^{21,22} Geometries of complexes were fully optimized by using default convergence criteria (energy change < 0.0005 hartree, atomic position displacement $< 0.005 \text{ \AA}$). Electron correlation was treated within the local density approximation (LDA) in the Vosko–Wilk–Nusair parametrization.²³ The nonlocal corrections (GGA) of Becke and Perdew were added to the exchange and correlation energies, respectively.²⁴ The analytical gradient method implemented by Versluis and Ziegler was used.²⁵ The standard ADF TZP basis set was used corresponding explicitly to a triple- ζ STO basis set for the valence core, augmented with a 2p polarization function for H, a 3d polarization function for C, N, and O, and a 6p polarization function for Pb and Bi. Orbitals up to 1s were kept frozen for C, N, and O, respectively. In the case of Pb and Bi, orbitals were frozen up to 4d.

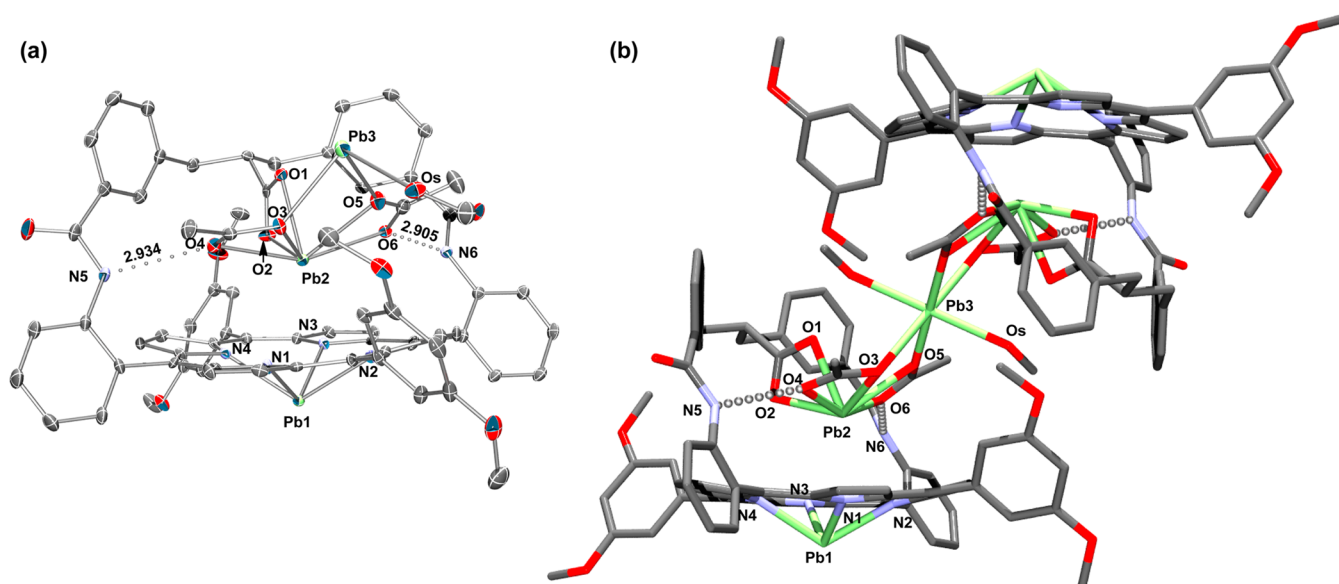


Figure 2. X-ray crystal structure of $[1_{\text{Pb}}\cdot\text{Pb}(\text{OAc})_2]_2\text{Pb}(\text{MeOH})_2$: (a) ORTEP view at 30% probability level of the asymmetric unit (hydrogen atoms omitted, dashed lines indicate H-bonds); (b) rod view of the pentanuclear complex; Os represents O atom from a methanol molecule. Distances [Å]: Pb2–Pb1 3.826; Pb2–Pb3 4.124; Pb1(/Pb2) to 24-atom mean plane 1.391(/2.390); Pb2–O1 2.435, Pb2–O2 2.454, Pb2–O3 2.724, Pb2–O4 2.580, Pb2–O5 2.642, Pb2–O6 2.577, Pb1–N1 2.422, Pb1–N2 2.408, Pb1–N3 2.393, Pb1–N4 2.404, Pb3–O3 2.507, Pb3–O5 2.490, Pb3–Os 2.515. Angles [deg]: (O1Pb2O2, O3Pb2O4) 77.17, (O1Pb2O2, O5Pb2O6) 78.75, (O3Pb2O4, O5Pb2O6) 27.62, (O3–Pb3–Os) 101.05, (O5–Pb3–Os) 89.02.

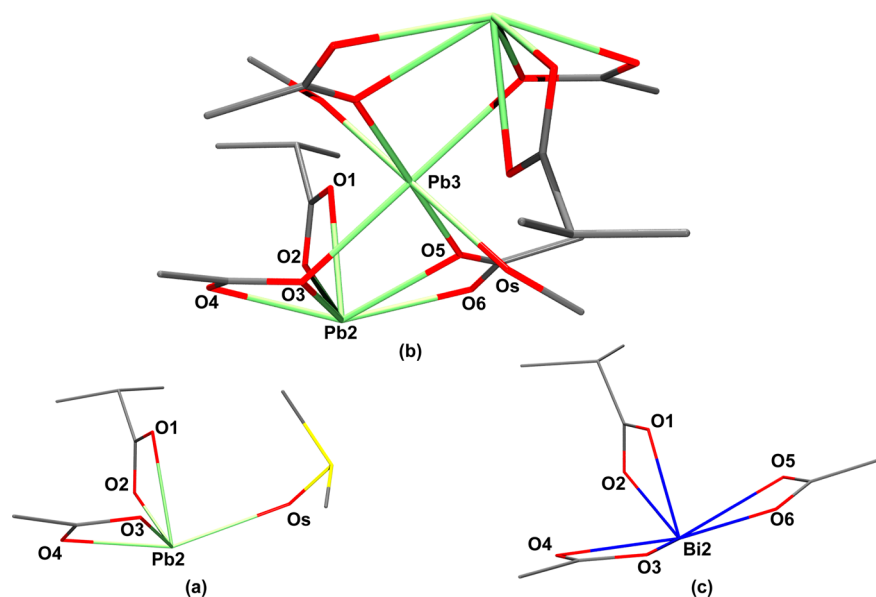


Figure 3. Rod representation of the polyhedron of coordination of the HAT cation in (a) $1_{\text{Pb}}\cdot\text{PbOAc}$,¹⁷ (b) $[1_{\text{Pb}}\cdot\text{Pb}(\text{OAc})_2]_2\text{Pb}(\text{MeOH})_2$, and (c) $2_{\text{Bi}}\cdot\text{Bi}(\text{OAc})_2$.¹⁴ Os represents O atom from (a) a DMSO molecule and (b) a methanol molecule.

RESULTS AND DISCUSSION

Porphyrin **1** was first titrated at 298 K with up to 5 equiv of $\text{Pb}(\text{OAc})_2$ in pyridine- d_5 (^1H NMR experiments, see the Supporting Information), which led to a two-step binding process very similar to what was observed previously in other solvents such as DMSO¹⁷ or $\text{CDCl}_3/\text{CD}_3\text{OD}$ mixtures.^{16a} It corresponds to the successive formation of a regular OOP mononuclear $\text{Pb}(\text{II})$ complex with the metal coordinated to the four nitrogen atoms of the porphyrin cavity, and the formation of the bimetallic complex $1_{\text{Pb}}\cdot\text{PbOAc}$ (Figure 1). No other binding event was detected. However, the X-ray crystallography analysis of single crystals obtained from the reaction of **1** with 5

equiv of $\text{Pb}(\text{OAc})_2$ in pyridine (see Experimental Section) revealed an unexpected dimeric assembly $[1_{\text{Pb}}\cdot\text{Pb}(\text{OAc})_2]_2\text{Pb}(\text{MeOH})_2$ (see Figure 2). This structure is centrosymmetric with lead atom Pb3 positioned at the center of symmetry. The edifice is a pentanuclear lead complex including two dinuclear lead(II) porphyrin units, very similar to $1_{\text{Pb}}\cdot\text{PbOAc}$ (Figure 1),¹⁷ assembled through a fifth lead atom. The latter exhibits a rather regular octahedral coordination polyhedron in which the four equatorial coordination sites are occupied by four acetate anions bound to the HAT metals of two porphyrins, whereas the two apical coordination sites are filled by two methanol molecules from the solvent of crystallization. Thus, the two

exogenous acetate anions of each porphyrin unit are shared between the HAT-bound lead cation Pb2 and the octahedral lead cation Pb3.

The asymmetric unit (Figure 2a) shows that the lead cation Pb1 is coordinated to the porphyrin macrocycle and located outside the cavity at 1.391 Å from the mean 24-atom porphyrin plane (24-MP). The second lead cation Pb2 is hanging inside the cavity of the strap. Pb2 coordinates the intramolecular carboxylate group from the strap and has no direct interaction with the macrocycle N-core (average Pb2–N distance 3.327 Å, slightly off-centered toward N1 (3.140 Å) and N2 (3.096 Å)). The position of Pb2 at 2.390 Å above the porphyrin 24-MP results in a long Pb1–Pb2 distance of 3.826 Å (95% of twice the lead van der Waals radius). A main difference with $\mathbf{1}_{\text{Pb}} \cdot \text{PbOAc}$ is the coordination of a second exogenous acetate group to Pb2 instead of a DMSO molecule. The 6-coordinate Pb2 is however characterized by an hemidirected coordination sphere of comparable extent relative to its 5-coordinate homologue in $\mathbf{1}_{\text{Pb}} \cdot \text{PbOAc}$ (Figure 3a,b), with a similar inward orientation of the metal. The acetate groups bound to Pb2 are still favorably oriented toward the amide groups of the strap. As a result, the hydrogen bonds (second sphere of coordination) with the acetate groups are quasi identical in both structures (2.92/2.93 Å vs 2.96 Å in $\mathbf{1}_{\text{Pb}} \cdot \text{PbOAc}$). However, the acetate groups linked to Pb2 are more weakly bound in the pentanuclear complex than in $\mathbf{1}_{\text{Pb}} \cdot \text{PbOAc}$ (O3(/O5)–Pb2 2.72(/2.64) Å vs 2.59 Å in $\mathbf{1}_{\text{Pb}} \cdot \text{PbOAc}$), and O4(/O6)–Pb2 is longer than in $\mathbf{1}_{\text{Pb}} \cdot \text{PbOAc}$ (2.58(/2.58) Å vs 2.43 Å) (see Table 1). It is also worth mentioning that both acetate groups are

Table 1. Distances (Å) and Angles (deg) of the HAT Cation M2 in $\mathbf{1}_{\text{Pb}} \cdot \text{PbOAc}$, $[\mathbf{1}_{\text{Pb}} \cdot \text{Pb}(\text{OAc})_2]_2 \text{Pb}(\text{MeOH})_2$, and $\mathbf{2}_{\text{Bi}} \cdot \text{Bi}(\text{OAc})_2$

	$\mathbf{1}_{\text{Pb}} \cdot \text{PbOAc}$	$[\mathbf{1}_{\text{Pb}} \cdot \text{Pb}(\text{OAc})_2]_2 \text{Pb}(\text{MeOH})_2$	$\mathbf{2}_{\text{Bi}} \cdot \text{Bi}(\text{OAc})_2$
O1–M2	2.45	2.43	2.21
O2–M2	2.38	2.45	2.49
O1–M2–O2	53.90	53.44	54.70
O3–M2	2.59	2.72	2.29
O4–M2	2.43	2.58	2.49
O3–M2–O4	51.50	49.26	54.93
CONH...O4	2.96	2.93	2.90
O5–M2	ne ^a	2.64	2.26
O6–M2	ne	2.58	2.55
O5–M2–O6	ne	49.98	53.26
CONH...O6	ne	2.92	2.84

^aNonexisting.

equally involved in the first sphere of coordination of Pb2 and in the second sphere of coordination with the strap (Table 1). They indeed possess the same short bond length (2.58 Å) for Pb2–O4 and Pb2–O6; the lengths of the longer bonds Pb2–O3 and Pb2–O5 are slightly different (2.72 and 2.64 Å). The two H-bonds between the acetate groups and the amide groups are also similar (2.92 Å vs 2.93 Å). Therefore, the two acetate groups cannot be distinguished. In addition, these two acetates further interact with the lead cation Pb3, as O3 and O5 bind Pb3 with almost equal bond lengths (2.51/2.49 Å). Therefore, these acetate groups act both as HAT-stabilizers via H-bonding for Pb2 and as bridging ligands between Pb2 and Pb3. The coordination sphere of Pb3 is completed by two axially bound methanol molecules.

The formal 2+ oxidation state of Pb3 could be controversial because the two protons from the methanol molecules were not observed in the X-ray diffraction map. Alternatively, Pb3 could be considered as a Pb(IV) cation with two methylate molecules and two acetate groups, although it would be difficult to rationalize which species could have abstracted the protons from methanol and could have oxidized the lead cation. To ascertain the oxidation state of the Pb3 atom, the bond valence sum (BVS) method²⁶ was first applied to calculate the valence of lead with the help of the *Bond_str* program.²⁷ By fitting a quite simple equation relating the oxidation state V_i of cation i to s_{ij} , the valence of the bonds between the cation i and the anions j , itself dependent on the bond length r_{ij} ,²⁸ and using the actual Pb–O interatomic distances obtained from the X-ray structure, a 2+ oxidation state of Pb3 can be proposed ($V_i = 1.99$). Identically, application of the BVS method to the Pb1 and Pb2 atoms leads to a formal 2+ oxidation state ($V_i = 2.27$ and 1.78, respectively). The 2+ oxidation state of Pb3 is confirmed by DFT calculations (see the Experimental Section for the computational details) because a large HOMO–LUMO gap (1.54 eV) is computed for $[\mathbf{1}_{\text{Pb}} \cdot \text{Pb}(\text{OAc})_2]_2 \text{Pb}(\text{MeOH})_2$ in the presence of two methanol molecules axially bound to Pb3. Indeed, calculations on the models $\text{Pb}(\text{MeOH})_2(\text{OAc})_4(\text{PbOAc})_2$ with two methanol molecules (Pb3(II); Figure 4a) extirpated from the pentanuclear complex $[\mathbf{1}_{\text{Pb}} \cdot \text{Pb}(\text{OAc})_2]_2 \text{Pb}(\text{MeOH})_2$ and $\text{Pb}(\text{OMe})_2(\text{OAc})_4(\text{PbOAc})_2$ with two methylate groups (Pb3-(IV)) indicate a large HOMO–LUMO gap only for the former (4.35 eV, that of the latter being only 0.04 eV) with a weakly Pb(6s)–O(2p) antibonding molecular orbital (MO) as the HOMO (see Figure 4b) close in energy to the occupied nonbonding ligand-localized MOs. This is a common situation for hexa-coordinated holo-directed Pb(II) complexes.^{5,29} Examination of the Voronoi net charges³⁰ shows that the holo-directed Pb3 atom is slightly more positive than the hemidirected Pb2 atoms (+1.952 and +1.635, respectively). Interestingly, atomic charges computed using the Voronoi method for the lead atoms in $[\mathbf{1}_{\text{Pb}} \cdot \text{Pb}(\text{OAc})_2]_2 \text{Pb}(\text{MeOH})_2$ show the same trend (+1.857, +1.711, and +1.426 for Pb3, Pb2, and Pb1, respectively).

The clear hemidirected configuration of the HAT Pb2 atom is associated with a rather large bond distance distribution, 0.290 Å (range: 2.435–2.725 Å, av 2.569 Å), whereas a much narrower bond distance distribution is observed for the holo-directed octahedral Pb3 atom, 0.035 Å (range: 2.490–2.525 Å, av 2.507 Å). It has been proposed that there is some relationship between the bond distance distribution and the gap size in the coordination sphere, that is, in the “void” in the angular distribution of ligands: the larger is the gap size, the larger is the bond distance distribution.²⁹ The presence of a “void” in the angular distribution of ligands around the hemidirected Pb2 atom correlates well with a stereochemically active lone pair of electrons. For comparison, the 5-coordinate HAT Pb2–O bond lengths are spread over 0.22 Å from 2.380 to 2.597 Å in $\mathbf{1}_{\text{Pb}} \cdot \text{PbOAc}$,¹⁷ and the 5-coordinate HAT Pb–O ones in $\mathbf{2}_{\text{Bi}} \cdot \text{PbOAc}$ ¹⁴ (see structure in Figure 1) stretch over 0.16 Å from 2.417 to 2.573 Å. This suggests a smaller influence of the lone pair of electrons for a smaller CN.

According to the valence bond theory, the inert electron-pair can either occupy a hybrid orbital formed by mixing the 6s and 6p orbitals on the metal ion and as such become stereochemically active, favoring hemidirected complexes, or be a pure 6s² electron pair and therefore stereochemically inactive, favoring

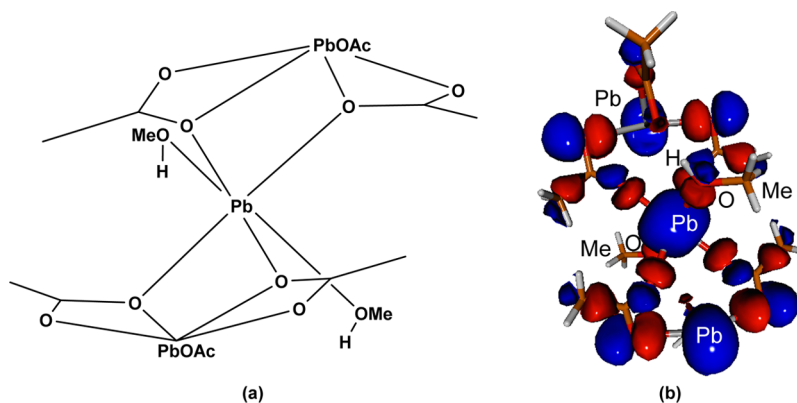


Figure 4. (a) Chemical structure and (b) HOMO of the model $\text{Pb}(\text{MeOH})_2(\text{OAc})_4(\text{PbOAc})_2$ used to mimic the Pb_3 environment in $[\mathbf{1}_{\text{Pb}} \cdot \text{Pb}(\text{OAc})_2]_2\text{Pb}(\text{MeOH})_2$ (isocontour value ± 0.02 [e/bohr^3] $^{1/2}$).

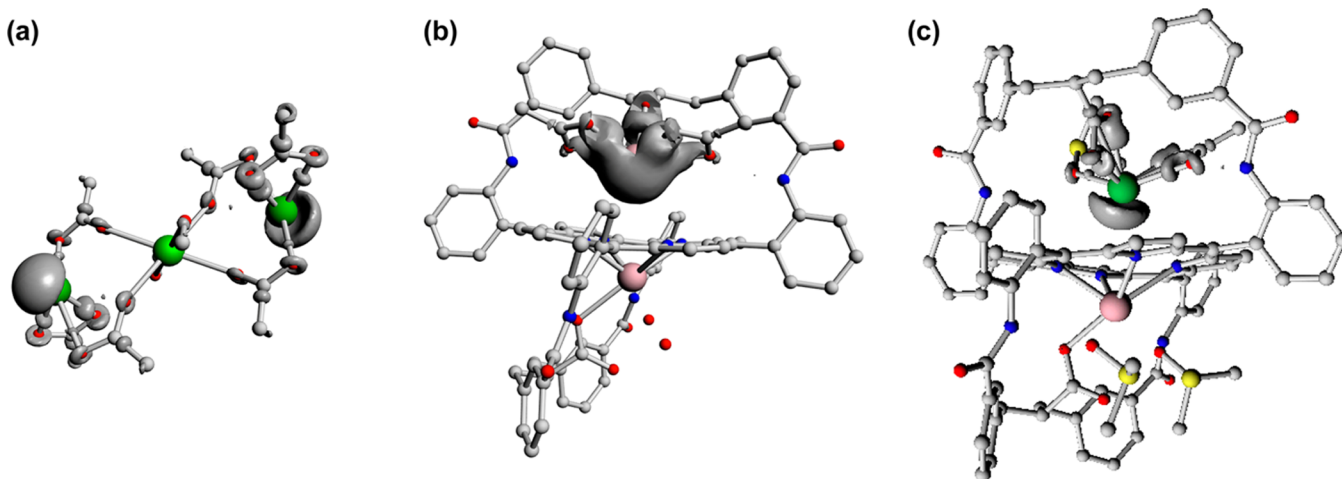


Figure 5. Deformation electron-density isosurface for the coordination spheres of (a) the hemidirected Pb_2 atom in the model $\text{Pb}(\text{MeOH})_2(\text{OAc})_4(\text{PbOAc})_2$, (b) the HAT Bi_2 in $2_{\text{Bi}} \cdot \text{Bi}(\text{OAc})_2$, and (c) the HAT Pb in $2_{\text{Bi}} \cdot \text{PbOAc}$ (DFT-optimized structures, the contour value is $+0.008$ e/bohr^3 ; hydrogen atoms have been removed for the sake of clarity).

holo-directed complexes.²⁹ However, according to molecular orbital theory, the classical concept of $6s/6p$ orbital hybridization on $\text{Pb}(\text{II})$ is considered incorrect because the energies and spatial distributions of these atomic orbitals are very dissimilar. The stereochemical activity observed in hemidirected lead(II) complexes should rather be seen as a result of antibonding lead $6s$ -ligand orbital interaction, which causes structural distortions to energetically minimize these unfavorable covalent interactions.^{5,31} In such complexes, the electron distribution around the metal ion can be unevenly distributed as was shown previously for $\mathbf{1}_{\text{Pb}} \cdot \text{PbOAc}$.¹⁷ To gain some information about the “volume” of electron density, which might hinder isotropic bond formation around the HAT hemidirected Pb_2 atom in the title compound, DFT calculations were carried out on the model $\text{Pb}(\text{MeOH})_2(\text{OAc})_4(\text{PbOAc})_2$. The lone pair of Pb_2 was then indirectly localized using the deformation electron-density map.³² The observed residual electron density in the vicinity of Pb_2 can be attributed to some *trans*-deformation of the lone pair orbital relative to the proximal OAc ligands (see Figure 5a), giving evidence of a stereochemically active lone pair of electrons comparatively to that in $\mathbf{1}_{\text{Pb}} \cdot \text{PbOAc}$. On the contrary, hardly any electron-density deformation is computed for the holo-directed Pb_3 atom, implying no stereochemical activity of the lone pair of electrons (Figure 6).

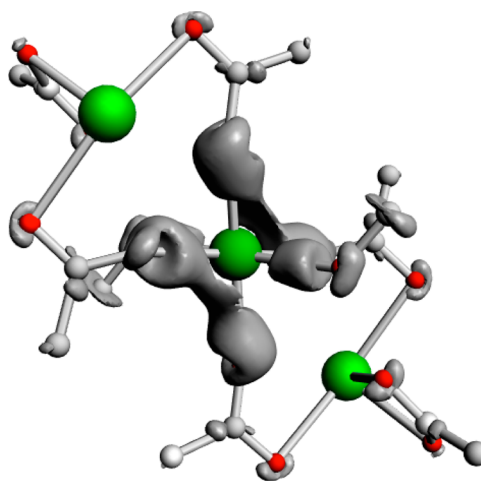


Figure 6. Deformation electron-density isosurface for the coordination sphere of the holo-directed Pb_3 atom in the model $\text{Pb}(\text{MeOH})_2(\text{OAc})_4(\text{PbOAc})_2$ (the contour value is $+0.005$ e/bohr^3 ; hydrogen atoms have been removed for the sake of clarity).

The pentanuclear porphyrin complex $[\mathbf{1}_{\text{Pb}} \cdot \text{Pb}(\text{OAc})_2]_2\text{Pb}(\text{MeOH})_2$ is a timely example of a supramolecular coordination edifice incorporating $\text{Pb}(\text{II})$ cations with three different

coordination modes: Pb1, hemidirected with N4 coordination sphere; Pb2, hemidirected with O6 coordination sphere; and Pb3, holo-directed with O6 coordination sphere. For Pb1, the large size of the cation relative to the porphyrin N-core and the lone pair activity associated with a low CN clearly impose an hemidirected coordination sphere. For Pb2 with intermediate CN (CN = 6), an hemidirected coordination sphere emerges from a combined effect of both the lone pair and the second sphere of coordination with the strap, although it is difficult to evaluate the extent of these two factors. For the 6-coordinate Pb3, although stabilizing interactions between the ligands (acetate binding to Pb2) could favor an hemidirected coordination sphere, the overcrowding that would result is probably the main factor that explains the holo-directed geometry.

Finally, it was interesting to compare the peculiar polyhedron of coordination observed for Pb2 in the pentanuclear lead complex $[1_{\text{Pb}}\cdot\text{Pb}(\text{OAc})_2]_2\text{Pb}(\text{MeOH})_2$ with that of bismuth(III) HAT cation Bi2 present in $2_{\text{Bi}}\cdot\text{Bi}(\text{OAc})_2$ (see Figure 1 bottom right and Figure 3b vs c; see also Table 1).^{4,14} Both HAT metals are 6-coordinate and possess very similar hemidirected coordination spheres: an intramolecular carboxylate group from the strap and two exogenous acetate groups stabilized by H-bonding with the two amide groups of the strap. In both complexes, these two H-bonds are of the same magnitude (Table 1), and the angles measured between the two exogenous acetate groups are only slightly different (154° in the case of Pb2 (O4–Pb2–O6) and 159° for Bi2 (O4–Bi2–O6)). This slight difference can be attributed to the bridging role (to Pb3) of the two exogenous acetate groups in $[1_{\text{Pb}}\cdot\text{Pb}(\text{OAc})_2]_2\text{Pb}(\text{MeOH})_2$. Besides, as mentioned above, it was shown that the bond distance distribution of the proximal ligands tethered to the post-transition metal cation is related to the volume of the nonspherical lone pair: the wider is the ligand–cation bond distance distribution, the larger is the volume.^{33,34} Pb2–O distances distribute over 0.29 Å from 2.435 to 2.725 Å in $[1_{\text{Pb}}\cdot\text{Pb}(\text{OAc})_2]_2\text{Pb}(\text{MeOH})_2$, whereas the Bi2–O distances distribute over 0.34 Å from 2.212 to 2.552 Å in $2_{\text{Bi}}\cdot\text{Bi}(\text{OAc})_2$.¹⁴ On the basis of these criteria, the “volume” of the lone pair of these HAT cations is expected to be nearly comparable, if not slightly larger, for Bi(III). As a comparison, in the hemidirected “butterfly shaped” structure of tris(3-hydroxy-2-methyl-4*H*-pyran-4-onato)bismuth(III), the Bi–O bonds distribute over 0.38 Å from 2.244 to 2.622 Å.³⁴

The deformation electron-density map for Bi2 in the DFT-optimized geometry of $2_{\text{Bi}}\cdot\text{Bi}(\text{OAc})_2$ was also computed and analyzed. As shown in Figure 5b, an electron-density pocket lies in the vicinity of Bi2, pointing away from the O atoms of the OAc ligands, in agreement with the presence of a stereochemically active lone pair of electrons contributing for the hemidirected geometry of Bi2 as it does for Pb2 in our model of $[1_{\text{Pb}}\cdot\text{Pb}(\text{OAc})_2]_2\text{Pb}(\text{MeOH})_2$. Interestingly, the nonspherical charge distribution around the HAT Bi(III) cation takes up more space than that around the HAT Pb(II) cation (Figure 5b vs a), which correlates well with the above-mentioned ligand–cation bond distance distributions. Similarly, the deformation electron-density map for the HAT Pb atom in $2_{\text{Bi}}\cdot\text{PbOAc}$ was also computed and is shown in Figure 5c. Visually, it appears that it is the smallest one in Figure 5, which is also in line with the smaller range of HAT Pb–O distances (0.16 Å, vide supra). Thus, in these particular HAT systems, both DFT and X-ray structures give a similar qualitative trend

for the “volume” of the lone pair: 6-coordinate Bi(III) > 6-coordinate Pb(II) > 5-coordinate Pb(II).

CONCLUSIONS

We have described here the first supramolecular assembly based on the interaction of a dinuclear lead porphyrin complex containing a HAT lead(II) cation. This assembly results from the coordination of an holo-directed octahedral lead(II) cation with two exogenous acetate residues shared with the hemidirected HAT Pb(II) metal of two porphyrin units, the OOP lead(II) cations remaining intact with respect to the supramolecular assembling process. DFT deformation electron-density maps show some pockets in the vicinity of the hemidirected HAT lead(II) atoms, which are associated with the presence of a stereochemically active lone pair of electrons. The comparison with other HAT systems shows that the “volume” of this lone pair correlates well with the bond distance distributions and the number of the proximal oxygen atoms tethered to the post-transition metal cation. Thus, the “volume” of this lone pair in the hexa-coordinate HAT Pb of $[1_{\text{Pb}}\cdot\text{Pb}(\text{OAc})_2]_2\text{Pb}(\text{MeOH})_2$ is slightly smaller than that in the hexa-coordinate HAT Bi in $2_{\text{Bi}}\cdot\text{Bi}(\text{OAc})_2$ and slightly larger than that of the penta-coordinate HAT Pb in $1_{\text{Pb}}\cdot\text{PbOAc}$ or $2_{\text{Bi}}\cdot\text{PbOAc}$. All in all, both the stereochemical activity of the lone pair and the second sphere of coordination of the ligands with the strap contribute to the hemidirected coordination of the HAT metals, either in 5- or in 6-coordinate.

Formally, the specific coordination of the HAT lead cation Pb2 allows an additional extension of the HAT coordination toward the assembling of several porphyrin units via coordination bonds with a third metal cation rather than just an adjunction through a bridging ligand. From this homopentanuclear complex, several extensions of this coordination chemistry can be envisaged with the octahedral lead replaced by another element that could be redox active. Investigations toward such developments are in progress in our laboratory.

ASSOCIATED CONTENT

Supporting Information

Crystallographic CIF file of $[1_{\text{Pb}}\cdot\text{Pb}(\text{OAc})_2]_2\text{Pb}(\text{MeOH})_2$ (CCDC-923915). ¹H NMR titration experiment of **1** with Pb(OAc)₂ in pyridine-*d*₅, and MOL file giving Cartesian coordinates of the computed complexes. This material is available free of charge via the Internet at <http://pubs.acs.org>.

AUTHOR INFORMATION

Corresponding Authors

*E-mail: stephane.legac@univ-rennes1.fr.

*E-mail: halet@univ-rennes1.fr.

*Tel.: +33(2)2323 5856. Fax: +33(2)2323 5637. E-mail: bernard.boitrel@univ-rennes1.fr.

Notes

The authors declare no competing financial interest.

ACKNOWLEDGMENTS

We gratefully acknowledge La Ligue contre le cancer, the ANR BLANC grant 12-BS07-0006-01, and Université Européenne de Bretagne for financial support.

REFERENCES

(1) Halime, Z.; Lachkar, M.; Furet, E.; Halet, J.-F.; Boitrel, B. *Inorg. Chem.* **2006**, *45*, 10661–10669.

- (2) Boitrel, B.; Breede, M.; Brothers, P. J.; Hodgson, M.; Michaudet, L.; Rickard, C. E. F.; Al Salim, N. *Dalton Trans.* **2003**, 1803–1807.
- (3) (a) Boitrel, B.; Halime, Z.; Michaudet, L.; Lachkar, M.; Toupet, L. *Chem. Commun.* **2003**, 2670–2671. (b) Lemon, C. M.; Brothers, P. J.; Boitrel, B. *Dalton Trans.* **2011**, 40, 6591–6609. (c) Boitrel, B. In *Biological Chemistry of Arsenic, Antimony and Bismuth*; Sun, H., Ed.; John Wiley & Sons, Ltd.: New York, 2011.
- (4) Rogers, R. D.; Bond, A. H.; Aguinaga, S.; Reyes, A. *J. Am. Chem. Soc.* **1992**, 114, 2967–2977.
- (5) Shimoni-Livny, L.; Glusker, J. P.; Bock, C. W. *Inorg. Chem.* **1998**, 37, 1853–1867.
- (6) (a) Boitrel, B.; Guillard, R. *Tetrahedron Lett.* **1994**, 35, 3719–3122. (b) Andrioletti, B.; Ricard, D.; Boitrel, B. *New J. Chem.* **1999**, 23, 1143–1150. (c) Michaudet, L.; Richard, P.; Boitrel, B. *Tetrahedron Lett.* **2000**, 41, 8289–8292. (d) Halime, Z.; Lachkar, M.; Toupet, L.; Coutsolelos, A. G.; Boitrel, B. *Dalton Trans.* **2007**, 3684–3689.
- (7) (a) Boitrel, B.; Halime, Z.; Balieu, S.; Lachkar, M. *C. R. Chim.* **2007**, 10, 583–589. (b) Le Gac, S.; Boitrel, B. *J. Porphyrins Phthalocyanines* **2012**, 16, 537–544.
- (8) (a) Michaudet, L.; Richard, P.; Boitrel, B. *Chem. Commun.* **2000**, 1589–1590. (b) Halime, Z.; Michaudet, L.; Lachkar, M.; Brossier, P.; Boitrel, B. *Bioconjugate Chem.* **2004**, 15, 1193–1200.
- (9) (a) Didier, A.; Michaudet, L.; Ricard, D.; Baveux-Chambenoit, V.; Richard, P.; Boitrel, B. *Eur. J. Org. Chem.* **2001**, 1917–1926. (b) Halime, Z.; Balieu, S.; Lachkar, M.; Roisnel, T.; Richard, P.; Boitrel, B. *Eur. J. Org. Chem.* **2006**, 1207–1215.
- (10) Liang, Y.; Chang, C. K. *Tetrahedron Lett.* **1995**, 36, 3817–3820.
- (11) Rosenthal, J.; Nocera, D. G. *Acc. Chem. Res.* **2007**, 40, 543–553.
- (12) The notation $\mathbf{1}_M$ refers to the location of a metal ion, bound out-of-plane to the N-core, on one or the other side of the macrocycle. For instance, $\mathbf{2}_{Bi}$ corresponds to an out-of-plane Bi(III) cation arbitrarily represented bound to the lower side of the porphyrin, as drawn in Figure 1. The C_2 -symmetrical complex $\mathbf{2Pb}_2$ represents an exception for this notation as each metal is OOP-bound to the N-core on each side of the macrocycle.
- (13) Halime, Z.; Lachkar, M.; Roisnel, T.; Furet, E.; Halet, J.-F.; Boitrel, B. *Angew. Chem., Int. Ed.* **2007**, 46, 5120–5124.
- (14) Najjari, B.; Le Gac, S.; Roisnel, T.; Dorcet, V.; Boitrel, B. *J. Am. Chem. Soc.* **2012**, 134, 16017–16032.
- (15) Le Gac, S.; Fusaro, L.; Dorcet, V.; Boitrel, B. *Chem.—Eur. J.* **2013**, 19, 13376–13386.
- (16) (a) Le Gac, S.; Najjari, B.; Dorcet, V.; Roisnel, T.; Fusaro, L.; Luhmer, M.; Furet, E.; Halet, J.-F.; Boitrel, B. *Chem.—Eur. J.* **2013**, 19, 11021–11038. (b) Le Gac, S.; Fusaro, L.; Roisnel, T.; Boitrel, B. *J. Am. Chem. Soc.* **2014**, 136, 6698–6715.
- (17) Le Gac, S.; Najjari, B.; Fusaro, L.; Roisnel, T.; Dorcet, V.; Luhmer, M.; Furet, E.; Halet, J.-F.; Boitrel, B. *Chem. Commun.* **2012**, 48, 3724–3726.
- (18) Altomare, A.; Burla, M. C.; Camalli, M.; Cascarano, G.; Giacovazzo, C.; Guagliardi, A.; Moliterni, A. G. G.; Polidori, G.; Spagna, R. *J. Appl. Crystallogr.* **1999**, 32, 115–119.
- (19) Sheldrick, G. M. *Acta Crystallogr.* **2008**, A64, 112–122.
- (20) Farrugia, L. J. *J. Appl. Crystallogr.* **1999**, 32, 837–838.
- (21) *ADF2012.01*; SCM, Theoretical Chemistry, Vrije Universiteit, Amsterdam, The Netherlands, <http://www.scm.com>.
- (22) te Velde, G.; Bickelhaupt, F. M.; van Gisbergen, S. J. A.; Fonseca Guerra, C.; Baerends, E. J.; Snijders, J. G.; Ziegler, T. *J. Comput. Chem.* **2001**, 22, 931–967.
- (23) Vosko, S. H.; Wilk, L.; Nusair, M. *Can. J. Phys.* **1980**, 58, 1200–1211.
- (24) (a) Becke, A. D. *Phys. Rev.* **1988**, A38, 3098–3200. (b) Perdew, J. P. *Phys. Rev. B* **1986**, 33, 8822–8824.
- (25) Verluise, L.; Ziegler, T. *J. Chem. Phys.* **1988**, 88, 322–328.
- (26) (a) O’Keeffe, M.; Brese, N. E. *J. Am. Chem. Soc.* **1991**, 113, 3226–3229. (b) Brese, N. E.; O’Keeffe, M. *Acta Crystallogr.* **1991**, B47, 192–197.
- (27) The *Bond_str* software is included in the FullProf Suite: www.ill.eu/sites/fullprof/; Rodriguez-Carvajal, J., 2012.
- (28) Brown, I. D.; Altermatt, D. *Acta Crystallogr.* **1985**, B41, 244–247.
- (29) Persson, I.; Lyczko, K.; Lundberg, D.; Eriksson, L.; Placzek, A. *Inorg. Chem.* **2011**, 50, 1058–1072.
- (30) Swart, M.; van Duijnen, P. Th.; Snijders, J. G. *J. Comput. Chem.* **2001**, 22, 79–88.
- (31) (a) Mudring, A.-V.; Rieger, F. *Inorg. Chem.* **2005**, 44, 6240–6243. (b) Walsh, A.; Watson, G. W. *J. Solid State Chem.* **2005**, 178, 1422–1428. (c) Mudring, A.-V. *Eur. J. Inorg. Chem.* **2007**, 882–890.
- (32) Deformation electron-density maps were obtained by subtracting from the molecular density of $Pb(MeO-H)_2(OAc)_4(PbOAc)_2$, the self-consistent computed densities of $[Pb]^{2+}$ (central lead) and $[(MeOH)_2(OAc)_4(PbOAc)_2]^{2-}$ units when considering the density around Pb3, while we used $[Pb]^{4+}$ (external lead atoms) and $[Pb(MeOH)_2(OAc)_4(OAc)_2]^{4-}$ units for investigations of the densities in the vicinity of the two Pb2 atoms. The fragment units were kept with their respective geometries in the model.
- (33) García-Montalvo, V.; Cea-Olivares, R.; Williams, D. J.; Espinosa-Pérez, G. *Inorg. Chem.* **1996**, 35, 3948–3953.
- (34) Sukhov, B. G.; Mukha, S. A.; Antipova, I. A.; Medvedeva, S. A.; Larina, L. I.; Chipanina, N. N.; Kazheva, O. N.; Shilov, G. V.; Dyachenko, O. A.; Trofimova, B. A. *ARKIVOC* **2008**, viii, 139–149.